

# Geostatistical Analysis of Field Spatial Distribution Patterns of Soybean Cyst Nematode

Felicitas Avendaño, Oliver Schabenberger, Francis J. Pierce, and Haddish Melakeberhan\*

## ABSTRACT

Site-specific management of soybean cyst nematode [*Heterodera glycines* Ichinohe] (SCN) is plausible if its spatial and temporal dynamics are adequately known and structured. The hypothesis that variation in the spatial distribution of SCN is sufficient in magnitude and structure and sufficiently time invariant to support the use of site-specific management in SCN-infested fields was tested. A nested survey sampling design with distances reduced by geometric progression was applied on two fields in Michigan. Cysts were extracted from single-core soil samples collected before planting in 1999 and 2000, the number of eggs per cyst was estimated, and the number of eggs per sample was obtained by multiplying eggs per cyst by the number of cysts. The distribution of the three variables was characterized using geostatistical tools such as semivariograms, kriging, and cross-correlograms on log-transformed values of the original data. Mean cyst population density ranged from 6 to 33 cysts 100 cm<sup>-3</sup> soil in the two fields. Although the spatial structure of SCN population varied between fields and SCN population density varied between years, the location of areas of high or low cyst density could be identified repeatedly. The reasons why nematodes exhibited an aggregated distribution are not yet understood. The evaluation of factors associated with the determination of SCN spatial distribution is part of an ongoing project toward the development of SCN site-specific management.

SOYBEAN CYST NEMATODE is a major pest of soybean [*Glycine max* (L.) Merr.] worldwide, accounting for approximately 54% (approximately  $1.67 \times 10^9$  U.S. dollars) of the soybean yield loss annually attributed to disease-causing agents in the United States (Wrather et al., 2001a, 2001b). Conducive cropping systems, highly adaptive behavior, and limited sources of resistance (Young, 1992; Young and Hartwig, 1992; Diers et al., 1999; Wang et al., 2000) are among the reasons SCN continues to be an economic threat. Eradication has been unsuccessful, and the repeated planting of resistant cultivars in the field results in the selection of a nematode population that can overcome plant resistance, reducing the longevity of the cultivar (Young, 1998). Thus, a realistic strategy for managing SCN appears to be through cultural-based practices for suppressing nematode populations (Bridge, 1996). An important consideration in managing SCN is that its aggregated distribution varies in space and time (Francl, 1986a, 1986b; Donald et al., 1999). The spatial-temporal variability in SCN is often overlooked in commonly used nematode-

sampling strategies that may miss field population clusters and in existing management thresholds that are based on whole-field sampling procedures. Thus, current SCN management practices involve treating whole fields rather than nematode-infested areas only and with uniform rather than condition-specific inputs. Advances in precision agriculture suggest that site-specific management of SCN is plausible but only if the spatial and temporal dynamics of SCN are adequately known and structured (Pierce and Nowak, 1999).

It is known that plant parasitic nematodes have aggregated spatial distribution with frequency distributions generally described by the negative binomial function (Anscombe, 1950; Seinhorst, 1982). Taylor's Power Law (Taylor, 1984) has been used to describe the distribution and to devise sampling strategies for nematodes (Ferris et al., 1990; McSorley and Dickson, 1991). Unfortunately, while recommendations call for systematic soil sampling to obtain samples that represent the entire area sampled (Ferris et al., 1990; McSorley and Dickson, 1991), samples are composited to form a single sample representative of the site average. Such spatially nonexplicit sampling is not conducive to examination of the possibility of site-specific management practices. The high cost of obtaining and analyzing nematode samples makes it imperative that methods of assessing spatial variability of SCN are highly effective and efficient. Efficiencies can be achieved through robust sampling designs or by relating SCN populations to more easily measured properties, such as soil pH or soil texture, that are known to have a somewhat structured spatial variation (Pierce and Nowak, 1999).

Geostatistics provide tools for describing spatial variation of soil properties and for local interpolation (kriging) to predict and map values at unsampled locations. Geostatistical methods can be applied to describe spatial autocorrelation of nematode distribution, soil properties, and host response to nematode infestation (Boag, 1998). While it is difficult to compare over a range of experimental conditions, variability in the spatial distribution of the cyst nematodes has been clearly demonstrated. A study on local variance of SCN using geostatistics showed that the scale of heterogeneity in the distribution of eggs between rows was similar to that within row (Francl, 1986a, 1986b). Webster and Boag (1992) showed that the levels of cereal cyst nematode (*Heterodera avenae*) and potato cyst nematode (*Globodera rostochiensis*) in soil are strongly autocorrelated at a normal working scale. Donald et al. (1999) found in a 4-yr field study that the spatial dependence in SCN egg population varied both within season and from season to season. In the field studied, the direction of spatial

F. Avendaño and H. Melakeberhan, Dep. of Entomol., 243 Natural Science Bldg., Michigan State Univ., East Lansing, MI 48824; O. Schabenberger, SAS Inst., Cary, NC 27513; and F.J. Pierce, Cent. for Precision Agric. Syst., Washington State Univ., 24106 North Bunn Rd., Prosser, WA 99350. Financial support for the project was provided by USDA Hatch Project through the Michigan Agricultural Experimental Station and grants from the Michigan Soybean Promotion Committee, North Central Soybean Research Program, and United Soybean Board to the last author. Received 6 Apr. 2002. \*Corresponding author (melakebe@msu.edu).

variation was related to the direction of tillage but not to other factors such as soil type or weed distribution (Donald et al., 1999). A better understanding of the spatial and temporal dynamics of the incidence of SCN would enable its more effective management by farmers. While previous studies clearly show the spatial dependence of SCN population density, more details are needed on the nature of spatial dependence and how it varies in adjacent fields and over time.

The objective of this work was to assess the magnitude, structure, and persistence in time of the spatial distribution patterns of SCN cysts, eggs, and eggs per cyst under field conditions using geostatistical tools. We hypothesize that the spatial distribution of SCN is sufficiently structured and time invariant to support the use of site-specific management in SCN-infested fields.

**MATERIALS AND METHODS**

**Experimental Sites and Site Management**

The study was conducted in Shiawassee County, MI, in 1999 and 2000 on two fields (Field A and Field B) located 3.2 km apart and maintained by the cooperating farmer. Field A was 24 ha, managed under no-tillage since 1996, and planted to corn (*Zea mays* L.) in 1998. Field B was 13 ha, conventionally tilled after wheat in 1998, and managed under no-tillage thereafter. A SCN-susceptible soybean variety ‘Asgrow 1901’

(Roundup Ready) was grown in both fields in 1999. Soybean was planted in 19.1-cm rows at a rate of 519 000 viable seeds ha<sup>-1</sup>. Row orientation was north-south in Field A and east-west in Field B. Fields A and B were planted within the same week in mid-May in 1999 and in early June in 2000, with planting delayed by wet soil conditions. Weed control was maintained using Roundup {[glyphosate [(N-(phosphonomethyl)glycine)]} at the recommended rate, with one preplant application in Field A in 1999 and 2000 and one application post-emergence in 1999. In Field B, there was one postemergence application in 1999 and one preplant application in 2000.

Soil series in Field A were Belding sandy loam (coarse-loamy, mixed, frigid Argic Endoaquods), Breckenridge sandy loam (coarse-loamy, mixed, nonacid, frigid Mollic Endoaquepts), Brookston loam (fine-loamy, mixed, superactive, mesic Typic Argiaquolls), Conover loam (fine-loamy, mixed, active, mesic Udollic Endoaqualls), and Newaygo sandy loam (fine-loamy over sandy or sandy-skeletal, mixed, frigid Alflic Haplorthods) (Fig. 1a). Soil series in Field B were Brookston loam, Newaygo sandy loam, and Berville loam (fine-loamy, mixed, mesic Typic Argiaquolls) (USDA-NRCS Soil Survey Div., 2001). Soil series maps were digitized from Threlkeld and Feenstra (1974) (Fig. 1b).

**Soil Sampling Design**

**1999**

A geostatistical sampling design was established in an 8-ha area and a 5.25-ha area in the center of Fields A and B,

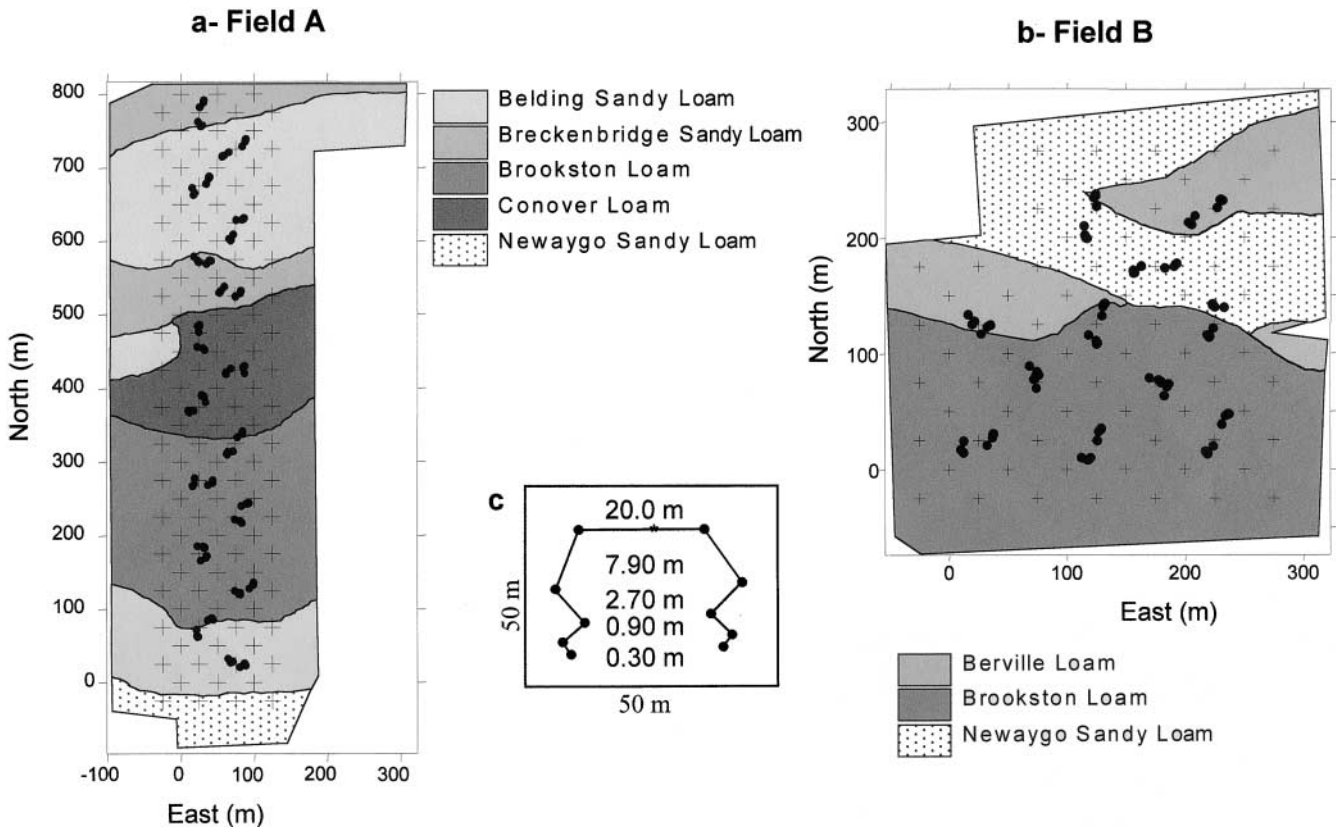


Fig. 1. Soil series maps and location of the soil samples collected from (a) Field A and (b) Field B in Shiawassee County, MI, in 1999 and 2000, and (c) nested sampling design with geometric progression-reduced distances. Distances between pairs of samples are indicated; the direction in which two consecutive samples were oriented was randomly selected. This design was applied within 50- by 50-m cells of a grid centered in each field. In Fig. 1a and 1b, black circles indicate sets of sample locations in selected cells for both 1999 and 2000, and the crosses indicate the locations of the additional samples collected in 2000 from alternate nodes of a 25- by 25-m grid. Soil series maps were digitized from Threlkeld and Feenstra (1974).

respectively (Fig. 1a and 1b). A grid of 50- by 50-m cells was marked on the area sampled. A nested survey sampling design with distances reduced by geometric progression (adapted from Webster and Boag, 1992) was applied to both fields within alternate cells of the grid. In each selected cell, a first pair of single-core samples was collected 20 m apart so that the segment connecting them passed through the center of the cell. A new point 7.9 m away from each sampled location was chosen in a random direction and also sampled. The procedure was repeated at 2.7, 0.9, and 0.3 m (Fig. 1c). The angles for each new location were randomly selected. Each angle was expressed in north and east coordinates to facilitate the location of the sampling sites in the field. This arrangement produced 10 sampling locations per cell that were flagged and georeferenced using GPS (Fig. 1a and 1b, black circles). The advantage of the nested survey design is to provide pairs of observations at various short- and long-range separation distances. This design guards against the potential pitfalls of regular grid-sampling designs when the shortest separation distance exceeds the range of the spatial process, in which case description of the spatial dependency structure of the spatial process would not be possible. Sampling locations were staked before harvest in 1999 to mark them for sampling in 2000.

## 2000

In addition to the 1999 sampling design, a grid with 25- by 25-m cells was superimposed on each field in 2000. The additional grid was added to expand the level of sampling detail because the nested design applied in 1999 provided very few pairs of samples for separation distances between 20 and 60 m. Soil samples were obtained from alternate nodes of the new grid, providing 119 and 77 additional samples from Fields A and B, respectively (Fig. 1a and b, crosses).

## Soil Sampling for Soybean Cyst Nematode

At each flag location, single-core soil samples were obtained within a week before planting using an 8-cm-diam. by 23-cm-depth bucket auger (Riverside Augers, Eijkelkamp, Giesbeek, the Netherlands). A total of 160 and 279 samples was collected from Field A and 110 and 187 samples were collected from Field B in 1999 and 2000, respectively. Soil cores were placed in individual plastic bags and, on arrival at the lab, were stored in 37.8-L (10-gallon) Rubbermaid containers at 4°C until they were processed (within 30 d).

## Cyst Extraction

Cysts were extracted by adding 100 mL of soil in a beaker containing 400 mL of tap water. A semiautomatic elutriator (Res. Serv. Instrument Shop, The Univ. of Georgia, Athens) was used for the extraction following standard procedures (Byrd et al., 1976) with 60% extraction efficiency (standard lab procedure). The last step in the elutriation process consists of the collection of nematodes and small soil particles suspended in water in a bowl. The bowl drains through 15 Tygon tubes into a 75- $\mu$ m aperture sieve (200 mesh) where cysts are retained. The volume of water and the amount of soil particles flowing from 15 tubes overflowed the sieve, so cysts were collected from seven tubes instead. Cysts collected in the sieve were further separated from soil particles following the sugar flotation–centrifugation method (Dunn, 1969). Cysts were then counted using a stereo microscope, and counts were adjusted to estimate the total number of cysts per sample if all 15 tubes had been used. Three cysts were randomly selected from each sample and crushed. Eggs and second-stage juve-

niles were counted using standard laboratory procedures. The average was used to determine the eggs per cyst for each sample containing at least one cyst. Egg numbers were estimated by multiplying the average number of eggs per cyst by the total number of cysts in each sample.

## Statistical Analysis

Soybean cyst nematode populations in Fields A and B were analyzed separately, and no statistical comparison was made between fields. For reasons beyond experimental control, a few samples were not collected from Fields A and B in 1999 or 2000. To compare populations between years, incomplete pairs (1999 or 2000 sample missing for a specific location) and additional data collected in 2000 were omitted only for the descriptive statistical analysis. Descriptive statistics for cysts, eggs per cyst, and eggs were calculated with the SAS System Release 8 (SAS Inst., Cary, NC). Histograms and cumulative distribution functions were plotted to compare the frequency distribution of cysts, eggs per cyst, and egg counts between years in each field. Logarithmic transformation of the data was performed whenever frequency distributions were highly skewed. Cumulative distribution functions for cysts [ $\log_{10}(\text{cysts} + 1)$ ], eggs [ $\log_{10}(\text{eggs} + 1)$ ], and eggs per cyst [ $\log_{10}(\text{eggs per cyst} + 1)$ ] were calculated and tested for log-normality with the Kolmogorov–Smirnov test, used to compare probability distributions to a specific function. Logarithmic-transformed means and sample variances were compared between years within fields with a paired *t* test and an *F* test, respectively ( $\alpha = 0.05$ ).

We used Taylor's Power Law to provide a measure of aggregation in SCN population density (Taylor, 1961, 1984; Ferris et al., 1990). Means and variances were computed from pairs of samples of cysts, eggs, and eggs per cyst, the samples being combined in different ways to give a range of spatial separations. The slope of the regression of log variance on log mean (parameter *b'*) was estimated by simple linear regression. Parameter *b'* is an index of aggregation, varying continuously from 0 for a regular distribution to 1 for a random distribution to  $\infty$  for a highly contagious distribution.

## Geostatistical Analysis

The semivariogram is a structural tool for depicting the spatial dependency in a realization of a mean–constant spatial process  $Z(\mathbf{s})$ . Attributes of interest for which semivariogram analysis was performed were the numbers of cysts, eggs per cyst, and egg population densities. Various estimators of the semivariogram are used in practice; Schabenberger and Pierce (2002) summarize several of these. Here, the classical Matheron estimator

$$\hat{\gamma}(h) = \frac{1}{2|N(h)|} \sum_{\|\mathbf{s}_i - \mathbf{s}_j\|=h} \{Z(\mathbf{s}_i) - Z(\mathbf{s}_j)\}^2$$

was used (Matheron, 1963). The semivariance  $\hat{\gamma}(h)$  at a given lag distance *h* is estimated as one-half the average squared difference between all observations at locations  $\mathbf{s}_i, \mathbf{s}_j$  that are separated by the *h*. The semivariogram for a given direction is displayed as a plot of  $\hat{\gamma}(h)$  versus distance. Depending on the data and sampling interval used, the shape of the experimental semivariogram may take many forms. In general, the semivariance increases with increasing distance between sample locations, rising to a more or less constant value (the sill) at a given separation distance called the range of spatial dependence. Samples separated by distances closer than the range are spatially related. Those separated by distances greater than the range are no longer spatially autocorrelated. Semivariances may also increase continuously without showing a defined

range and sill, thus preventing definition of a spatial variance, indicating that the range is greater than the largest lag (*h*) or the presence of a trend effect and/or nonstationarity (Webster and Burgess, 1980). Stationarity means that the random field sampled looks similar everywhere. A random field is second-order stationary if the mean of the random field is constant and does not depend on locations, and the covariance between two observations is only a function of their spatial separation (Schabenberger and Pierce, 2002). Whenever semivariograms showed nonstationarity, the data were detrended by carrying out a polynomial least-squares regression, and semivariogram analysis was performed on the residuals. Other semivariograms show complete absence of spatial structure, implying that the value observed at one location carries no information about values at other locations. The nugget effect (*C*<sub>0</sub>) is a discontinuity of the semivariance near the origin. It consists of measurement error variability and/or the sill of a microscale spatial process. The error variance is a measure of repeatability of the data measurements, whereas microscale variance is a measure of variation that occurs at separation distances less than the smallest sample spacing (Cressie, 1993).

To reduce the influence of extreme values and to achieve greater symmetry, log-transformed data were used for the geostatistical analysis. Experimental omnidirectional semivariograms of cysts [ $\log_{10}(\text{cysts} + 1)$ ], eggs per cyst [ $\log_{10}(\text{eggs per cyst} + 1)$ ], and eggs [ $\log_{10}(\text{eggs} + 1)$ ] were calculated for each field and year for lags ranging from 1 to 30 m, with a lag tolerance of one-half of the lag used (*h*/2). The minimum number of pairs required for each lag was 30. The reduced number of samples in the east–west direction in Field A and the predominant southwest–northeast arrangement of the samples in Field B prevented the calculation of reliable directional semivariograms. Variography was performed with the Surfer 7.02 software package (Golden Software, 1999).

Kriging is the best linear unbiased prediction of regionalized variables at unsampled locations using the structural properties of the semivariogram and the sampled values at observed locations. Soil properties often exhibit lognormal probability distributions, in which case log-Gaussian kriging is employed. It involves computation of semivariograms and kriging on log-transformed values of the original data using the same procedures as for simple linear kriging (Cressie, 1993). When

a drift or trend (nonstationarity of the mean) existed within the area of interest, universal kriging was used; otherwise, ordinary kriging was the method of choice. Universal kriging takes the drift into account, provided the form of the drift and the semivariogram are known (Journel and Huijbregts, 1978). The distributions of cysts, eggs, and eggs per cyst were mapped separately for each field and year with ordinary or universal log-kriging predicting values at the nodes of a 1- by 1-m cell grid using all of the data points in each sample and the parameters from the models fitted to the empirical semivariograms.

The cross-correlogram is used to describe the spatial continuity between measurements of different attributes or of the same attribute measured at different times. The cross-correlation function given by Goovaerts (1997) was used here to calculate cross-correlograms for logarithmic-transformed cysts, eggs per cyst, and eggs between years and for logarithmic-transformed eggs per cyst and eggs in 1999 with cysts in 2000. Only the data points from locations sampled in both 1999 and 2000 were used for this analysis.

## RESULTS

### Population Densities of Soybean Cyst Nematode

Cyst and egg population densities of SCN, as well as eggs per cyst, varied significantly between fields and years. Cyst population density for entire fields ranged from as low as 6 cysts 100 cm<sup>-3</sup> soil in Field A in 1999 to as high as 33 cysts 100 cm<sup>-3</sup> soil in Field B in 2000. The lowest and the highest egg population densities were also found in Field A in 1999 (87 eggs 100 cm<sup>-3</sup> soil) and in Field B in 2000 (4939 eggs per 100 cm<sup>-3</sup> soil), respectively (Table 1).

#### Field A

While mean cyst density in Field A remained similar and low in 1999 and in 2000, with positively skewed frequency distribution (Table 1 and Fig. 2a), the sample variance of cyst density increased significantly in 2000

**Table 1. Summary statistics of soybean cyst nematode (SCN) cyst and egg population densities and eggs per cyst from two fields in Shiawassee County, MI, before planting in 1999 and 2000.**

	Cysts		Eggs†		Eggs per cyst‡	
	1999	2000	1999	2000	1999	2000
Counts 100 cm <sup>-3</sup> soil						
<b>Field A</b>						
Arithmetic mean§	6.4 NS	8.4 NS	86.6*	851.5*	13.0*	48.9*
Standard deviation¶	6.56*	10.8*	129.2*	1571.4*	20.6*	48.2*
CV, %	102	129	149	184	158	98
Min.–max.	0–41	0–69	0–656	0–8369	0–270	0–168
Sample size#	157	157	115	115	115	115
<i>b'</i> value (SE)††	1.4 (0.03)	1.5 (0.03)	1.6 (0.02)	2.0 (0.03)	1.8 (0.02)	1.4 (0.05)
<b>Field B</b>						
Arithmetic mean§	14.5*	32.9*	2442.6*	4938.7*	116.5*	87.9*
Standard deviation¶	22.1*	58.2*	3531.5*	8975*	58.8 NS	69.7 NS
CV, %	152	176	144	182	50	79
Min.–max.	0–121	0–484	0–17 368	0–68 284	0–298	0–285
Sample size#	109	109	79	79	79	79
<i>b'</i> value (SE)††	1.7 (0.03)	1.7 (0.03)	2.1 (0.04)	1.8 (0.02)	1.1 (0.13)	0.9 (0.06)

\* Significance at the 0.05 probability level.

† Egg density in each sample was estimated by multiplying the average number of eggs per cyst by the total number of cysts found in the sample.

‡ The number of eggs per cyst is the average number of eggs counted after crushing three randomly selected cysts in each sample.

§ Arithmetic means of logarithmic-transformed data were compared between years using the paired *t* test. Arithmetic means of original data are shown for clarity.

¶ Sample variances of logarithmic-transformed data were compared between years using the *F* test. Standard deviations of original data are shown for clarity.

# Sample size for analyses of eggs and eggs per cyst include only samples with at least one cyst.

†† Taylor's Power Law index of aggregation *b'* and standard error (SE).

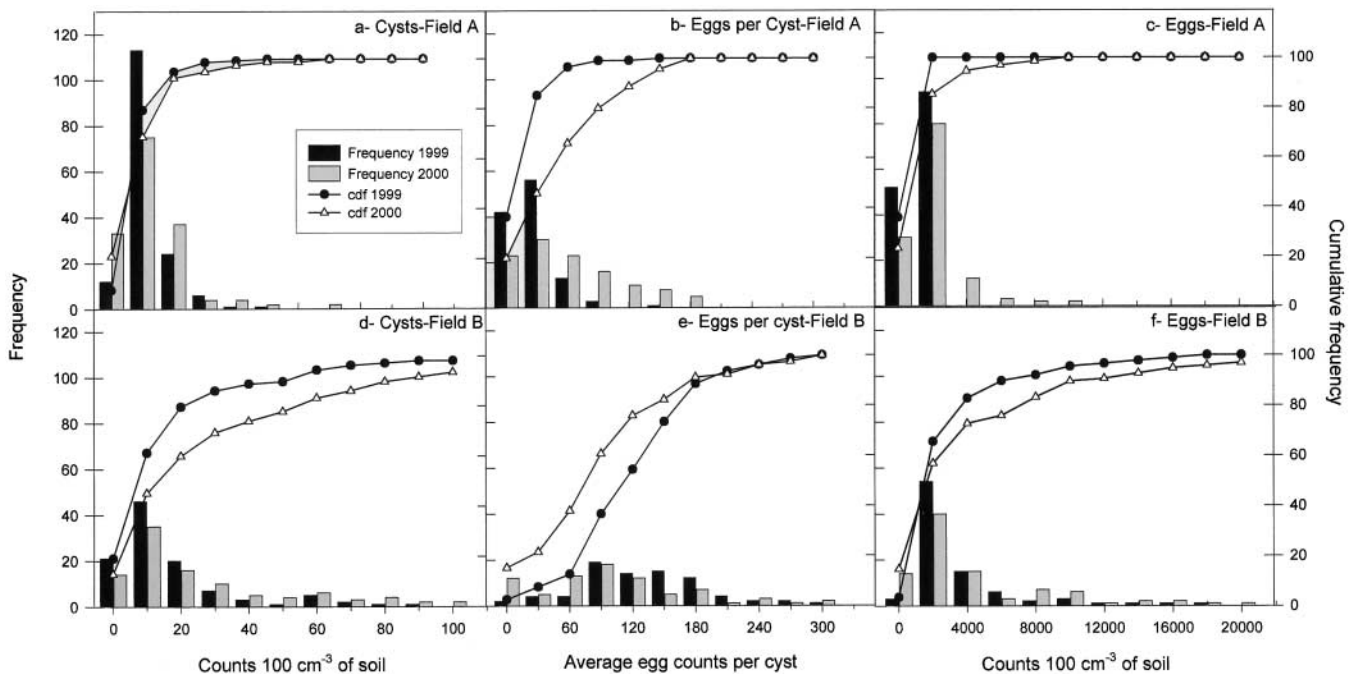


Fig. 2. Frequency distribution and cumulative distribution function (cdf) of (a) cysts  $100 \text{ cm}^{-3}$  soil, (b) eggs per cyst, and (c) eggs  $100 \text{ cm}^{-3}$  soil from Field A and (d) cysts  $100 \text{ cm}^{-3}$  soil, (e) eggs per cyst, and (f) eggs  $100 \text{ cm}^{-3}$  soil from Field B. Samples were collected before planting in 1999 and 2000. The number of eggs per cyst was estimated as the average number of eggs found after crushing three randomly selected cysts in each sample.

(Table 1). Taylor's Power Law index of aggregation  $b'$  indicated a moderately aggregated distribution of cysts in 1999 and 2000. Mean egg density and sample variance were significantly higher in 2000 than in 1999 as a result of the increased production of eggs per cyst in 2000 (Table 1; Fig. 2b and 2c). The degree of aggregation in the population of eggs was also greater in 2000 than in 1999, whereas the opposite was true for the number of eggs per cyst (Table 1). The proportion of cysts without eggs decreased from 36% in 1999 to 23% in 2000, indicating that more cysts had eggs at planting and, therefore, that there was a greater infection potential in 2000 (Fig. 2b).

### Field B

Soybean cyst nematode population density in Field B was moderate in 1999 and high in 2000. The mean number of cysts found in 2000 was 2.3 times greater than in 1999, with greater variability as well (Table 1). The distribution of relative frequencies was positively skewed in both years (Fig. 2d). In 1999, cysts were not detected in 19.3% of the samples, whereas in 2000, this proportion decreased to 13.6% (Fig. 2d). The same moderate degree of aggregation in cyst population was observed in 1999 and 2000 (Table 1). The number of eggs found in 2000 was significantly greater and more variable than in 1999 (Table 1 and Fig. 2f). In contrast to Field A, the production of eggs per cyst was reduced by 25% from 1999 to 2000 (Table 1), and 13.7% of the cysts were without eggs in 2000 compared with only 2.3% in 1999 (Fig. 2e). Therefore, the increase in egg density in 2000 was due to the greater number of cysts and not to increased egg production. Taylor's index of

aggregation indicated aggregation in egg population and insufficient evidence of aggregation in the number of eggs per cyst in 1999 and 2000 (Table 1). Relative frequency distributions of eggs per cyst appeared normal in both years, with medians (109 eggs cyst<sup>-1</sup> in 1999 and 75 eggs cyst<sup>-1</sup> in 2000) close to the means (113 eggs cyst<sup>-1</sup> in 1999 and 86 eggs cyst<sup>-1</sup> in 2000) (Fig. 2e).

### Geostatistical Analysis

Although the spatial structure of SCN population density varied between fields and years, the spatial autocorrelation in cyst and egg population densities, as well as eggs per cyst, was structured to a lesser degree in 2000 than in 1999. Empirical semivariograms were calculated and graphed for lags ranging from 3 to 30 m, but only those calculated for a lag of 10 m were selected for modeling because they represented more clearly the structure of the spatial variability in these fields. The models fitted and their corresponding parameter estimates are given in Table 2.

### Field A

The data exhibited nonstationarity in mean for logarithmic-transformed cyst data in 1999 (data not shown). Therefore, the semivariogram was calculated with the residuals after a polynomial trend was removed. The experimental semivariograms of cyst density in 2000, and egg density and eggs per cyst in both years showed stationarity in the distribution (Fig. 3b–3f). Empirical semivariograms clearly showed periodicity in the spatial structure of the distribution of cysts, eggs, and eggs per cyst (Fig. 3a–3f). However, because of the large nugget

**Table 2. Parameters of the theoretical semivariogram models of soybean cyst nematode (SCN) population density in two fields in Shiawassee County, MI, before planting in 1999 and 2000.†**

	Drift‡	Model function	C₀§	C¶	Range#	C₀/(C + C₀)††
<b>Field A 1999</b>						
Cysts‡‡	Linear	Nugget	0.08		m	0.50
		Wave		0.04	3.6	
		Spherical		0.04	819.3	
Eggs per cyst§§	No	Nugget	0.34			0.77
		Spherical		0.1	168.3	
Eggs¶¶	No	Nugget	0.8			0.77
		Wave		0.24	4.5	
<b>Field A 2000</b>						
Cyst	No	Nugget	0.18			0.69
		Spherical		0.08	122	
Eggs per cyst	No	Nugget	0.33			0.44
		Wave		0.41	7.13	
Eggs	No	Nugget	1.32			
<b>Field B 1999</b>						
Cysts	Linear	Nugget	0.07			0.35
		Wave		0.13	12.16	
Eggs per cyst	No	Nugget	0.08			0.44
		Wave		0.1	11.93	
Eggs	No	Nugget	0.25			0.43
		Wave		0.33	10.22	
<b>Field B 2000</b>						
Cyst	Linear	Nugget	0.09			0.37
		Wave		0.08	2.62	
		Spherical		0.07	268	
Eggs per cyst	No	Nugget	0.44			
Eggs	No	Nugget	1.1			0.86
		Wave		0.18	4.24	

† Models were fitted by least squares based on empirical semivariograms calculated for lags (*h*) ranging from 1 to 25 m, with a lag tolerance of *h*/2. The minimum number of pairs required for each lag was 30.

‡ Whenever semivariograms showed nonstationarity, the data were detrended carrying out a simple polynomial least-squares regression, and semivariogram analysis was performed on the residuals. The polynomial order of the trend is indicated when a drift or trend was removed.

§ C₀ is the nugget effect or a discontinuity in semivariance at the origin due to microscale variability or sampling error.

¶ C is the partial sill defined for spherical models.

# Observations that are spatially separated by more than the range are uncorrelated.

†† C₀/(C + C₀) is an indicator of the degree of spatial structure—the lower the number is, the stronger the spatial autocorrelation.

‡‡ Semivariograms for cysts were calculated for log₁₀(cysts 100 cm⁻³ soil + 1). Cysts were extracted from a 100-cm³ soil subsample with a semiautomatic elutriator and counted.

§§ Semivariograms of eggs per cyst were calculated for log₁₀(eggs per cyst + 1). The number of eggs per cyst was estimated as the average number of eggs counted after crushing three randomly selected cysts in each sample.

¶¶ Semivariograms for eggs were calculated for log₁₀(eggs 100 cm⁻³ soil + 1). Egg density was determined for each sample by multiplying the average number of eggs per cyst by the number of cysts in the sample.

effect in some cases, a wave- or hole-effect model could not be fitted (Fig. 3b, 3c, and 3f). The empirical semivariogram of cysts in 1999 showed two scales of spatial structure: one described by a wave-effect model with a short range indicating the presence of small clusters of cysts and the second by a spherical model with a much greater range describing the spatial autocorrelation of those smaller clusters (Fig. 3a). A similar pattern was observed in 2000 although the periodicity could not be modeled in this case (Fig. 3b). The semivariance of eggs per cyst increased with increasing lag distance up to a range of almost 170 m in 1999 (Fig. 3c). In 2000, a wave-effect model with a range of 7 m described the periodicity in the distribution of eggs per cyst (Fig. 3d). The semivariance for eggs fluctuated about the sample variance with increasing separation distance between data pairs in 1999 and 2000, indicating a clustered distribution of eggs within a very short range, even though a wave-effect model could not be fitted in 2000 because of the large nugget (first lag represented by 131 pairs) (Fig. 3e–3f).

**Field B**

The data exhibited nonstationarity in mean for logarithmic-transformed cyst data in both years (data not

shown). Therefore, semivariograms were calculated from residuals after removal of a polynomial trend. In 1999, the distribution of cysts showed strong spatial autocorrelation described by a wave-effect model with a range of 12 m (Fig. 4a). In 2000, the structure of the empirical semivariogram was similar to the one observed for cysts in Field A in 1999. A wave-effect model and a spherical model described the short- and long-range structures, respectively (Fig. 4b). The periodicity observed in the empirical semivariograms of eggs per cyst and eggs could be described by wave-effect models, except for eggs per cyst in 2000 where the nugget effect was too large (174 pairs in the first lag) (Fig. 4c–4f). These semivariograms indicate clustered distribution of eggs and eggs per cyst.

**Kriging**

The distributions of cysts, eggs, and eggs per cyst were mapped separately for each field and year with ordinary or universal log-kriging using the parameters from the models fitted to the experimental semivariograms (Table 2).

The distribution of cysts in Field A varied slightly from 1999 to 2000. In 1999, small clusters of cysts were aggregated in larger patches. Cyst density was lower in

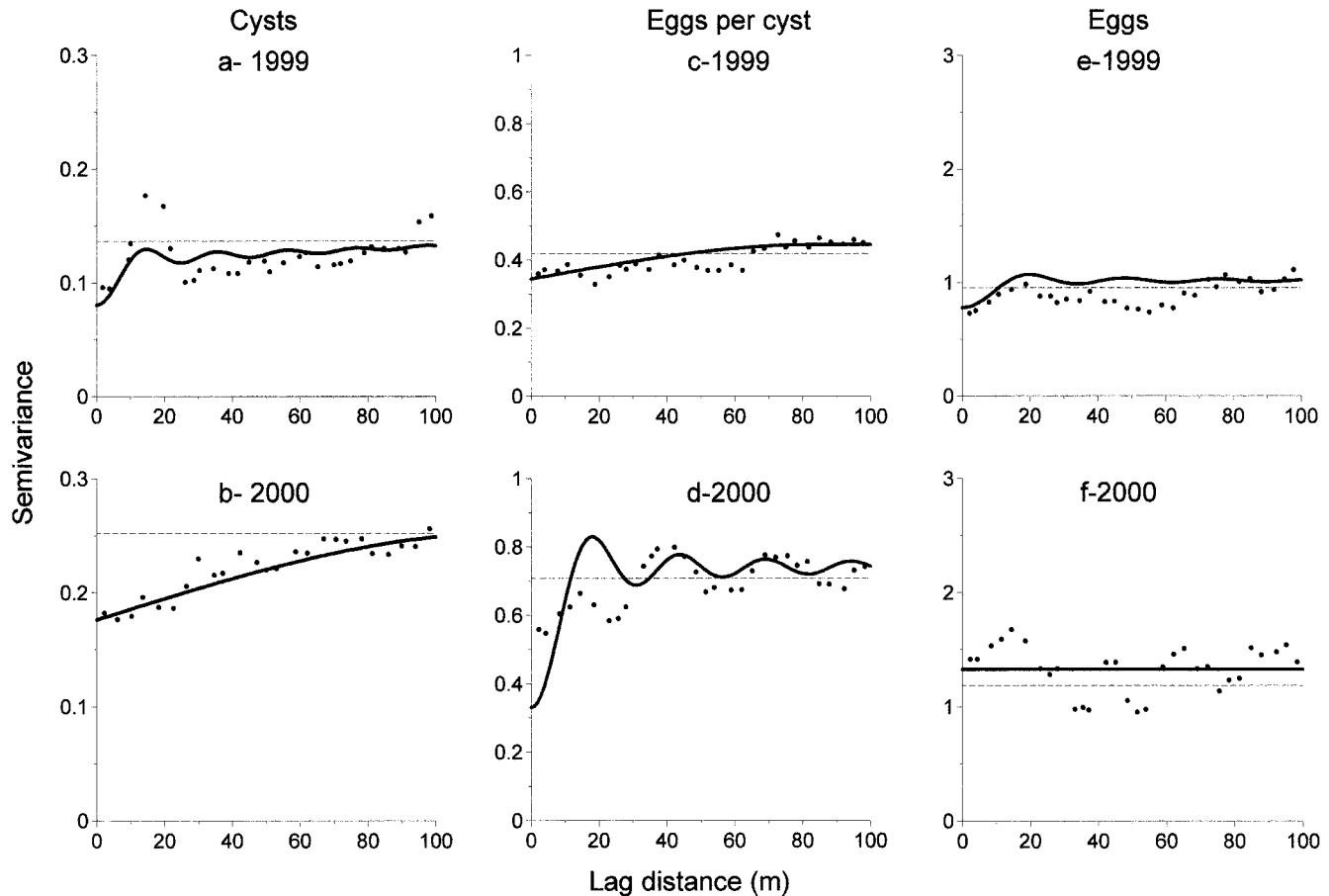


Fig. 3. Semivariograms of (a and b) cysts [ $\log_{10}(\text{cysts } 100 \text{ cm}^{-3} \text{ soil} + 1)$ ], (c and d) eggs per cyst [ $\log_{10}(\text{eggs per cyst} + 1)$ ], and (e and f) eggs [ $\log_{10}(\text{eggs } 100 \text{ cm}^{-3} \text{ soil} + 1)$ ] from Field A in (a, c, and e) 1999 and (b, d, and f) 2000. Black circles indicate omnidirectional empirical semivariogram, the solid line indicates the theoretical model fitted by means of least squares, and the dashed line is the sample variance.

the center of the area sampled and in the north end. The highest cyst density was found in the south portion of the field and in a band of approximately 100 m wide located between 550 and 650 m north (Fig. 5a). In 2000, cyst density increased throughout the field, and the distribution pattern changed in some portions of the field when compared with the pattern observed in 1999 (Fig. 5b). Even though the grouping in small clusters disappeared, cyst density remained low in the center and the northwest corner of the field. The most significant change in the distribution was observed in the southeast corner of the field where cyst density decreased markedly in 2000. Despite the similarities in cyst distribution between years, the cross-correlogram indicated weak correlation between cysts in 1999 and 2000 for very short lags and no cross-correlation beyond a separation distance of 20 m (Fig. 6a). The poor spatial structure and the low number of eggs per cyst in 1999 generated a distribution of kriged values rather uniform throughout the field (Fig. 5c). The increased number in eggs per cyst and cysts with eggs in 2000 may have contributed to a better defined spatial structure. Kriged values for eggs per cyst in 2000 showed small clusters of high and low values distributed randomly throughout the field (Fig. 5d). The distribution of high and low egg density areas resembled that of cysts in 1999 (Fig. 5e). Because

of the nature of the semivariogram model (pure nugget effect), the map of egg distribution in 2000 represented the egg mean density throughout the field (not shown). The distribution of eggs per cyst and eggs were uncorrelated between 1999 and 2000 (Fig. 6b and 6c). Cyst population density at planting in 2000 was poorly correlated with eggs per cyst or eggs at planting the previous year (Fig. 7a and 7b).

The distribution of cysts in Field B indicated the presence of a well-defined area with high cyst density located in the northeast corner and an area with low cyst density in the southwest corner of the sampled site in 1999. Clusters of high and low cyst density were mixed in between these extreme locations (Fig. 8a). The pattern was maintained in 2000 with a relatively high linear correlation coefficient (Fig. 6d), but the infected area was larger, extended toward the south, and did not include low-density clusters (Fig. 8b). The cross-correlogram for cysts between years showed a decrease in correlation as the separation distance between samples increased (Fig. 6d). Patches of eggs-per-cyst density slightly higher than the mean were distributed throughout the field in 1999, with the lowest numbers located on the southeast corner of the site (Fig. 7c). In 2000, the distribution of eggs produced per cyst was represented by the mean throughout the field because of the

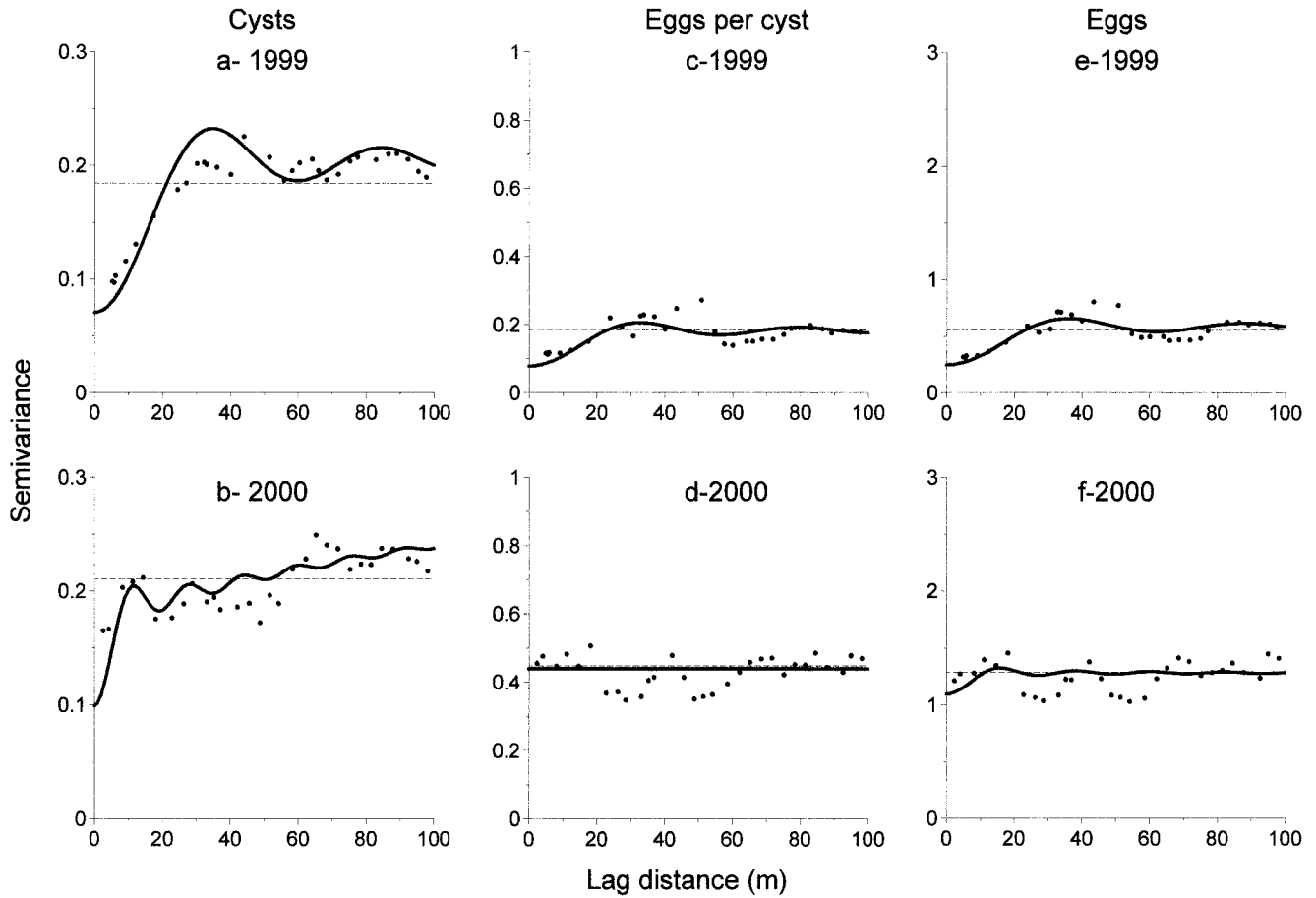


Fig. 4. Semivariograms of (a and b) cysts [ $\log_{10}(\text{cysts } 100 \text{ cm}^{-3} \text{ soil} + 1)$ ], (c and d) eggs per cyst [ $\log_{10}(\text{eggs per cyst} + 1)$ ], and (e and f) eggs [ $\log_{10}(\text{eggs } 100 \text{ cm}^{-3} \text{ soil} + 1)$ ] from Field B in (a, c, and e) 1999 and (b, d, and f) 2000. Black circles indicate omnidirectional empirical semivariogram, the solid line indicates the theoretical model fitted by means of least squares, and the dashed line is the sample variance.

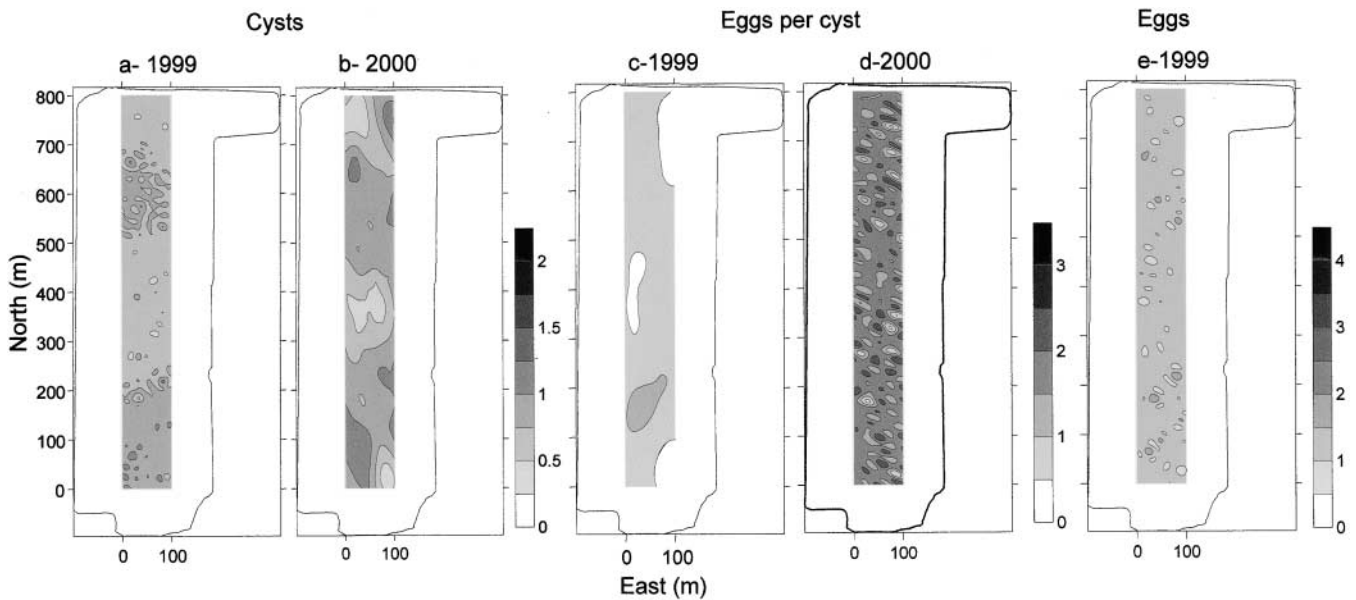


Fig. 5. Log-kriged maps represent the distribution of cysts in the area sampled within Field A in (a) 1999 and (b) 2000, the distribution of eggs per cyst in (c) 1999 and (d) 2000, and the distribution of eggs in (e) 1999. The shading scale indicates levels of cysts [ $\log_{10}(\text{cysts } 100 \text{ cm}^{-3} \text{ soil} + 1)$ ], eggs per cyst [ $\log_{10}(\text{eggs per cyst} + 1)$ ], and eggs [ $\log_{10}(\text{eggs } 100 \text{ cm}^{-3} \text{ soil} + 1)$ ]. A solid line delineates the field boundaries.

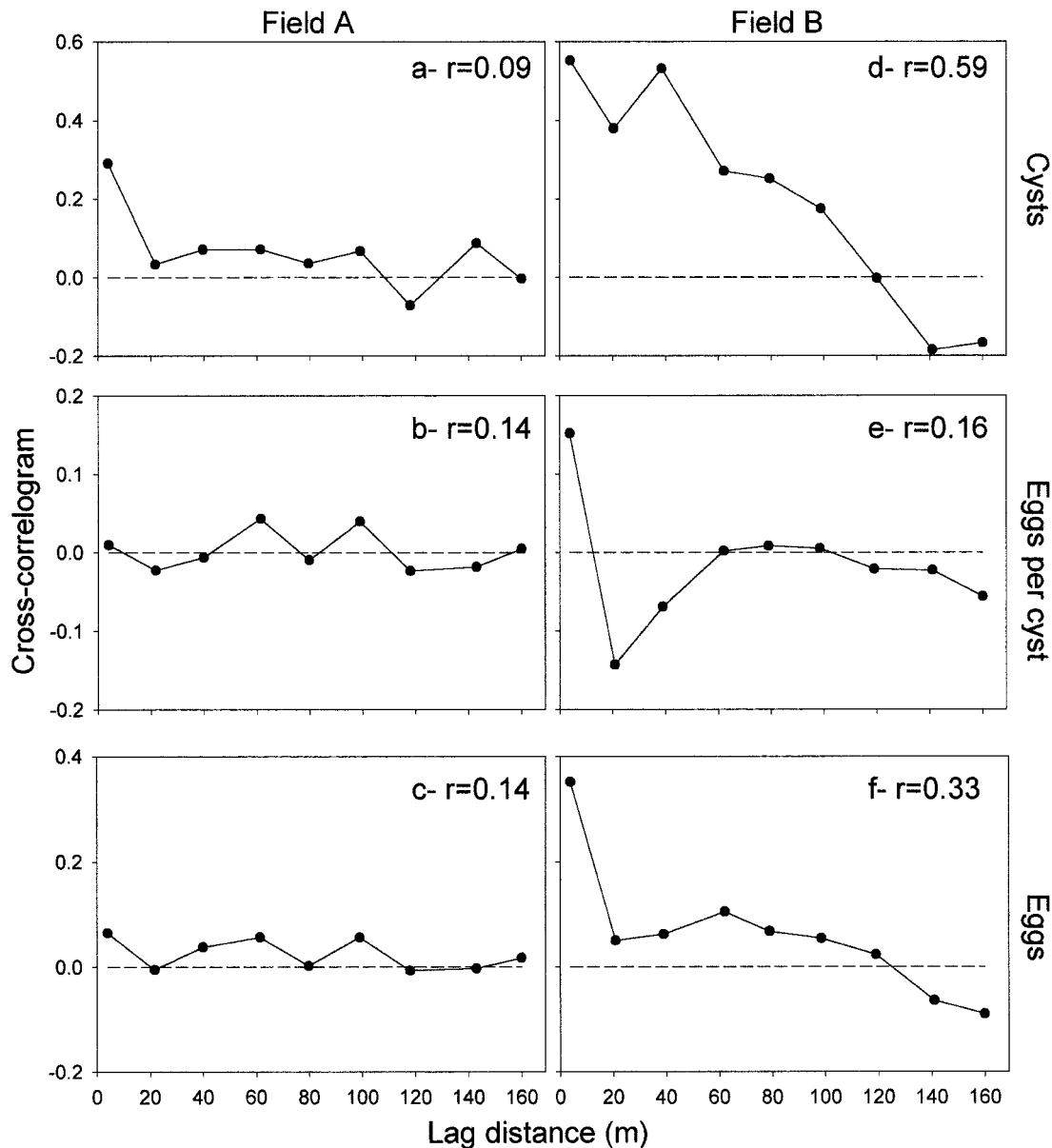


Fig. 6. Cross-correlograms between (a and d) cysts [ $\log_{10}(\text{cysts } 100 \text{ cm}^{-3} \text{ soil} + 1)$ ], (b and e) eggs per cyst [ $\log_{10}(\text{eggs per cyst} + 1)$ ], and (c and f) eggs [ $\log_{10}(\text{eggs } 100 \text{ cm}^{-3} \text{ soil} + 1)$ ] in 1999 and 2000 in (a, b, and c) Field A and (d, e, and f) Field B.  $r$  = linear correlation coefficient.

nature of the semivariogram model (not shown). The distribution of eggs matched well that of cysts in 1999 and 2000 as expected because the number of eggs is a linear function of cysts and eggs per cyst and the coefficient of variation (CV) of cysts was much greater than the CV of eggs per cyst (Fig. 8d and 8e; Table 1). In 1999, it was possible to identify clusters of spatial autocorrelation in the distribution of eggs, whereas in 2000, the clusters appear to merge into more homogeneous bands. The correlation in the distribution of eggs per cyst between years was poor at short lags, becoming negative with increasing separation distance and nonexistent beyond 60 m (Fig. 6e). The distribution of eggs was moderately correlated between years at very short lags and uncorrelated beyond 20 m (Fig. 6f). Cyst population density in 2000 was poorly correlated with the number of eggs per cyst in 1999 but relatively well corre-

lated with egg density at planting in 1999 (Fig. 7c and 7d).

## DISCUSSION

The objective of this work was to assess the magnitude, structure, and persistence in time of the spatial distribution patterns of SCN cysts, eggs, and eggs per cyst under field conditions using geostatistical tools. Geostatistics have been used to study the spatial distribution of soil-inhabiting plant pathogens such as fungus-vectoring viruses (Workneh et al., 2001), soil nematode community structure (Robertson and Freckman, 1995), and cyst nematodes under semicontrolled and field conditions (Francl, 1986a, 1986b; Webster and Boag, 1992; Evans et al., 1998; Donald et al., 1999, 2001). In almost all cases, spatial patterns have been demonstrated. How-

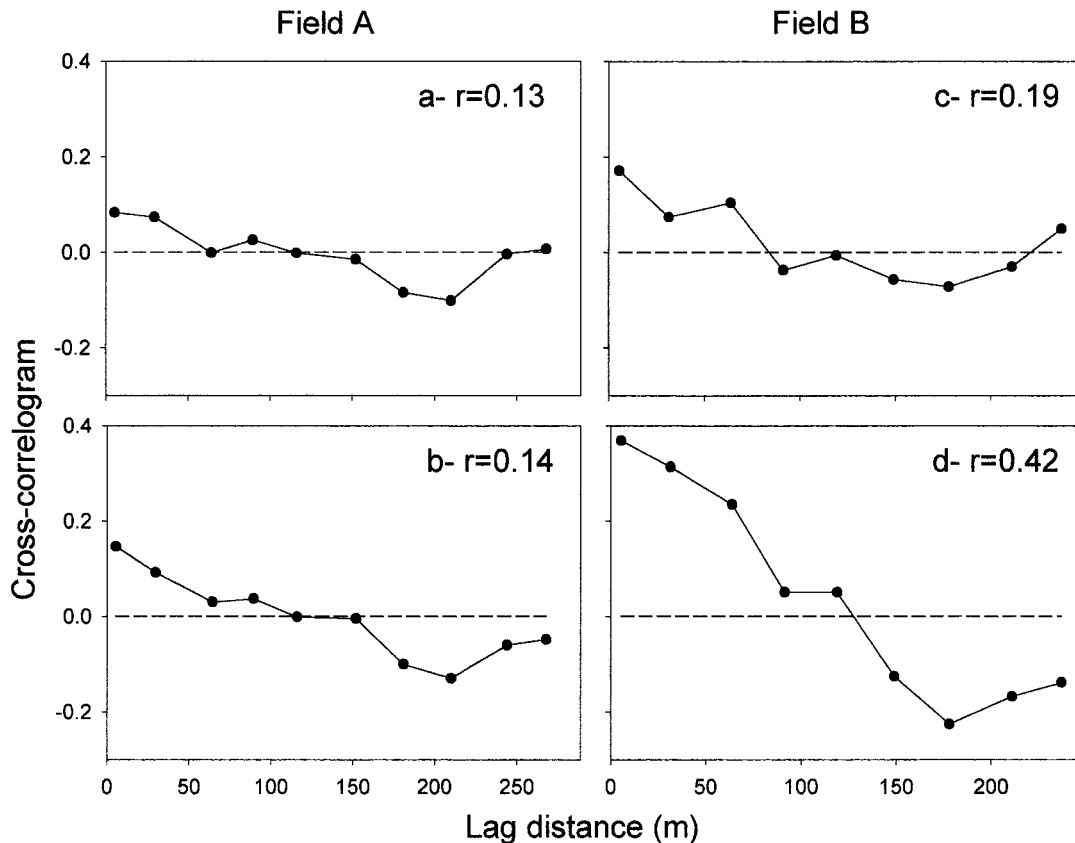


Fig. 7. Cross-correlograms between (a and c) eggs per cyst [ $\log_{10}(\text{eggs per cyst} + 1)$ ] in 1999 and cysts [ $\log_{10}(\text{cysts } 100 \text{ cm}^{-3} \text{ soil} + 1)$ ] in 2000 and (b and d) eggs [ $\log_{10}(\text{eggs } 100 \text{ cm}^{-3} \text{ soil} + 1)$ ] in 1999 and cysts in 2000 in (a and b) Field A and (c and d) Field B.  $r$  = linear correlation coefficient.

ever, the precision of defining the spatial structure seems to vary with the type of sampling design used. The sampling design selected for this study allowed for the construction and analysis of detailed semivariograms for short separation distances, thus contributing to the understanding of SCN spatial distribution patterns. A regular grid may provide more uniform coverage of the area to be sampled, but the scale of spatial autocorrelation may be missed if the distance between nodes is larger than or equal to the range of the semivariogram. For exploratory spatial analysis, the nested sampling design of Webster and Boag (1992) has an advantage over regular grids in that it provides information for a variety of short separation distances (lags), thus enabling the analysis of the structure of the semivariogram when the scale of spatial variability is unknown. Taylor's Power Law has been used to determine the degree of aggregation of many nematode species (Boag and Topham, 1984; Duncan et al., 1989; Ferris et al., 1990; McSorley and Dickson, 1991; Webster and Boag, 1992). While the index of aggregation  $b'$  was not affected by sample size (Boag and Topham, 1984), it differed by species and by the separation distance between samples (Boag and Topham, 1984; Webster and Boag, 1992). In Fields A and B, Taylor's index of aggregation did not correspond with the information obtained from the semivariograms on the spatial structure in SCN population. This might be due to the periodicity encountered in

SCN population, with positive and negative correlation between samples as the separation distance increased. A plot of Taylor's index  $b'$  vs. separation distance between samples would probably have reflected the fluctuations observed in the empirical semivariograms.

The spatial distribution of SCN cysts, eggs, and eggs per cyst exhibited varying degrees of aggregation and structure, and the spatial structure varied between years. While the exact causes of varied SCN spatial distribution are poorly understood, nematode multiplication and population density equilibrium are influenced by host-nematode interactions and the prevailing environmental conditions (Seinhorst, 1967). For example, SCN reproduction and subsequent survival could be influenced by nonhost plants or the presence of a resistant cultivar (Riggs, 1987). These, in turn, may lead to a less structured and more random distribution of the surviving cysts in soils. Hence, the low number of SCN cysts observed in Field A before planting in 1999 appears to be the outcome of corn, a nonhost crop, grown the previous year, thereby possibly explaining the poorly structured spatial distribution observed for cysts in Field A in 1999. When infective juveniles hatch where a susceptible soybean variety is grown, SCN can complete several generations during a growing season, and population density can increase sharply if conditions are adequate (Lauritis et al., 1983; Bonner and Schmitt, 1985). Soybean cyst nematode population densities that were below the de-

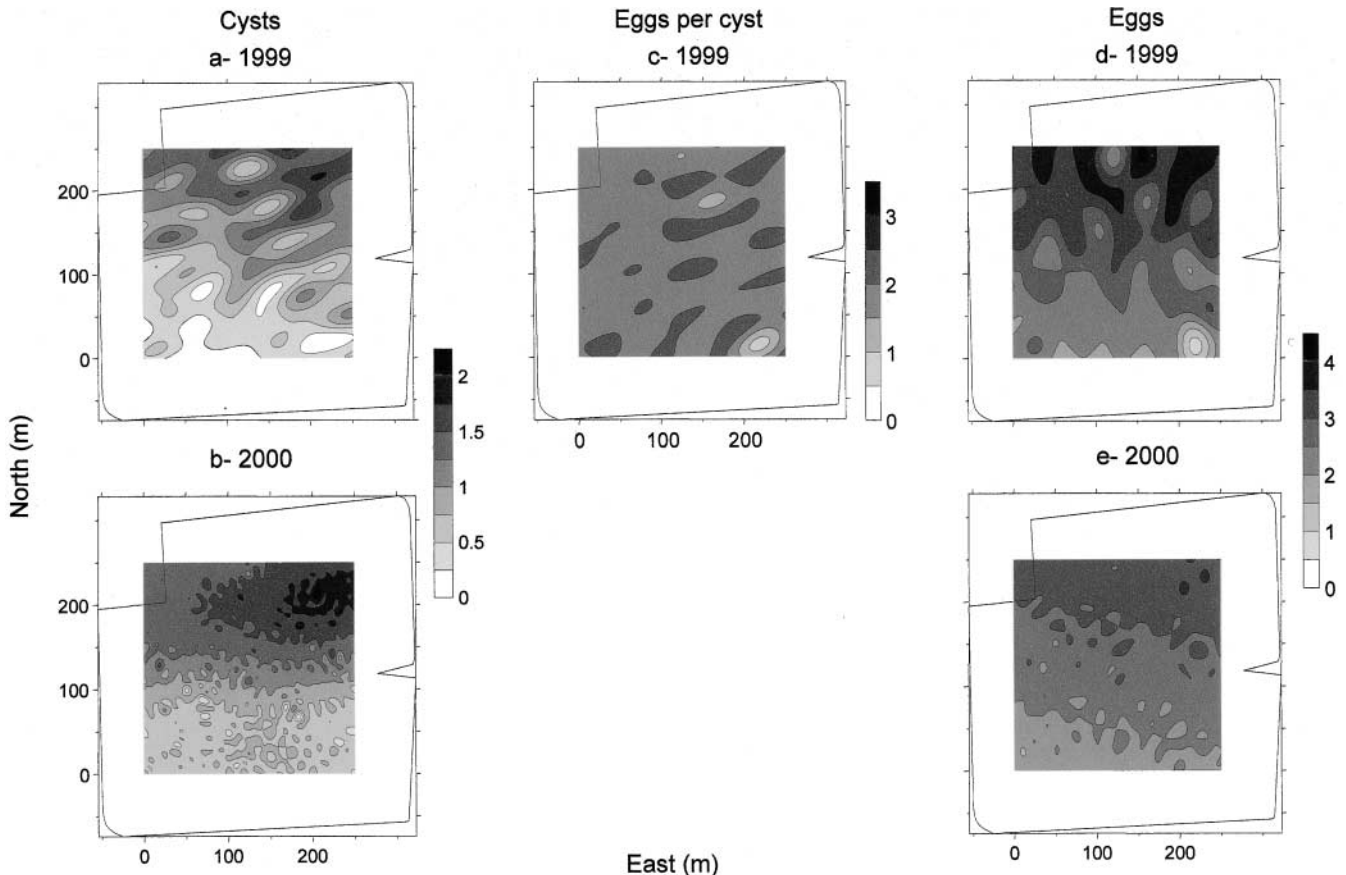


Fig. 8. Log-kriged maps represent the distribution of cysts in the area sampled within Field B in (a) 1999 and (b) 2000, the distribution of eggs per cyst in (c) 1999, and the distribution of eggs in (d) 1999 and (e) 2000. The shading scale indicates levels of cysts [ $\log_{10}(\text{cysts } 100 \text{ cm}^{-3} \text{ soil} + 1)$ ], eggs per cyst [ $\log_{10}(\text{eggs per cyst} + 1)$ ], and eggs [ $\log_{10}(\text{eggs } 100 \text{ cm}^{-3} \text{ soil} + 1)$ ]. A solid line delineates the field boundaries.

tection limit at planting in 1999 may have increased to detectable levels in 2000 after susceptible soybean, generating changes in the spatial structure poorly correlated between years. The cysts and eggs distribution maps in Field B showed that the areas with more eggs in 1999 resulted in increased cyst density in 2000, and areas with fewer eggs in 1999 resulted in relatively fewer cysts in 2000 (Fig. 8), indicating a positive correlation based on spatial location between eggs at planting and cyst density the following spring. This correlation was corroborated by the cross-correlogram (Fig. 7d). Over time, and under adequate conditions, the spatial distribution of cysts in this field, and possibly in Field A too, may become more structured.

Plant parasitic nematodes act as sinks of photoassimilates and nutrients, and their ability to function as such will vary considerably depending on their physiological age (Bird and Loveys, 1975). Soybean cyst nematode females are more likely to reach maturity in primary rather than in secondary or tertiary roots; thus, maturity may be related to the distance between the infection site (the sink) and the shoot (Melton et al., 1986). Plants with large root biomass offer more feeding sites to nematodes, favoring infection but not necessarily improved egg production. In Field B, we observed that the soybean plants located in the area where cyst and egg densities were high grew more poorly than plants in areas

with lower nematode densities. At the same time, cysts located in the northeast corner of the field contained similar numbers of eggs in 2000 as cysts found in areas with healthier plants (pure nugget effect semivariogram). Soil properties are very likely also involved in this relationship (Koenning et al., 1988; Todd and Pearson, 1988; Koenning and Barker, 1995). Among other factors, poor growth could be a function of soil moisture where generally more, deeper, and less evenly distributed roots develop under drought stress, offering more feeding sites to nematodes (Huck et al., 1986). The portion of the field where plants grew poorly was well drained (Newaygo sandy loam), suggesting that drought stress may have been an adverse factor for plant growth in addition to the abundance of SCN. These observations correspond with those of Koenning and Barker (1995) where plant growth was adversely affected in coarse soils with poor water-holding capacity even when there was a continuous water supply. A combination of causal factors could result in patches of cyst density and variation of egg production, thereby generating spatial autocorrelation over time and in the presence of a suitable host.

Although strong winds, farming equipment, animals, and flooding may disperse eggs and cysts in a field or move them to new locations, the most common dispersal mechanism of SCN is movement of soil (Lehman, 1994).

Even though both fields were in no-tillage management between 1999 and 2000 with a residue coverage protecting the soil, some SCN movement is possible. For example, soil peds containing eggs and cysts adhered to the residue may have been moved by the wind and by planting and harvesting operations. In addition, the surface run-off in the spring of 2000 may have altered previously existent spatial structure toward a more uniform pattern.

Earlier reports indicated a strong relationship between the spatial distribution of SCN and soil texture (Workneh et al., 1999; Donald et al., 2001). In this study, variations in soil properties are likely to have had the most influence on SCN spatial structures and trends observed, especially in Field B. The influences may have been direct on the nematode population density, indirectly mediated through the host, or a combination of both.

The site-specific management of SCN is plausible because SCN studies have shown that it is not uniformly distributed within fields and because the cost and performance of eradication practices suggest that management offers the most viable control option for SCN. To make site-specific SCN management successful, the spatial distribution of SCN must be highly structured and temporally stable within a given field. In the fields evaluated in this study, the within-field variability in cysts and eggs per cyst was large ( $CV > 100\%$ ), but spatial variability was weakly structured as evidenced by high nugget variances and poor fit of semivariogram models. Poor spatial structure and the high cost of sampling nematodes make the success of site-specific management in these fields unlikely. However, although there was poor correlation in cyst density between years in Field A, the temporal variability in SCN distribution was small. There were areas within each field in which SCN was not detected or occurred at only low density, and the areas of high or low SCN population density remained approximately at the same locations between years. We also know from remote sensing and yield maps (not presented here) that soybean performance was correlated with SCN infection. Therefore, the notion of SCN management zones, areas in which different SCN management practices would be applied, could be a viable option if appropriate criteria for the delineation of effective management zones were determined. Deriving and evaluating delineation criteria of SCN management zones is a continuing goal of this research effort.

#### ACKNOWLEDGMENTS

The project is part of a Ph.D dissertation of the first author. We gratefully acknowledge anonymous reviewers for their helpful comments and criticisms, which improved the quality of the manuscript. We thank Chad Holovach, Nathan Nye, Megan Kierzek, Carolyn Stein, Nathan Cottrell, Bindiya Shah, Dan Armstrong, Marisol Soto, Carolina Holteuer, Katrina Blakely, and Teresa Raslich for assistance in collecting and processing samples and Dave Eickholt, Charles Eickholt (farmers), and Neil R. Miller (ABC-Agribusiness Consultant) for providing and maintaining the sites.

#### REFERENCES

- Anscombe, F.J. 1950. Soil sampling for potato root eel worm cysts. *Ann. Appl. Biol.* 37:286–295.
- Bird, A.F., and B.R. Loveys. 1975. The incorporation of photosynthates by *Meloidogyne javanica*. *J. Nematol.* 7:111–113.
- Boag, B. 1998. Survey, surveillance and crop loss assessment. p. 123–140. *In* S.B. Sharma (ed.). *The cyst nematodes*. Kluwer Academic Publ., London.
- Boag, B., and P.B. Topham. 1984. Aggregation of plant parasitic nematodes and Taylor's Power Law. *Nematologica* 30:348–357.
- Bonner, M.J., and D.P. Schmitt. 1985. Population dynamics of *Heterodera glycines* life stages on soybean. *J. Nematol.* 17:153–158.
- Bridge, J. 1996. Nematode management in sustainable and subsistence agriculture. *Annu. Rev. Phytopathol.* 34:201–225.
- Byrd, D.W., Jr., K.R. Barker, H. Ferris, C.J. Nusbaum, W.E. Griffin, R.H. Small, and C.A. Stone. 1976. Two semi-automatic elutriators for extracting nematodes and certain fungi from soil. *J. Nematol.* 8:206–212.
- Cressie, N.A.C. 1993. *Statistics for spatial data*. Revised ed. J. Wiley and Sons, New York.
- Diers, B.W., P. Arelli, and S.R. Cianzio. 1999. Management of SCN through conventional breeding for resistance—Midwest perspective. p. 5. *In* Proc. Natl. Soybean Cyst Nematode Conf., Orlando, FL. 7–8 Jan. 1999. United Soybean Board, Orlando, FL.
- Donald, P.A., W.W. Donald, A.J. Keaster, R.J. Kremer, J.A. Kendig, B.S. Sims, and J. Mihail. 1999. Changes in *Heterodera glycines* egg population density in continuous *Glycine max* over four years. *J. Nematol.* 31:45–53.
- Donald, P.A., K.A. Sudduth, and N.R. Kitchen. 2001. Mapping soybean cyst nematode field distribution. *Phytopathology* 91:S133 (abstr.).
- Duncan, L.W., J.J. Ferguson, R.A. Dunn, and J.W. Noling. 1989. Application of Taylor's Power Law to sample statistics of *Tylenchulus semipenetrans* in Florida citrus. *J. Nematol.* 21:707–711.
- Dunn, R.A. 1969. Extraction of cysts of *Heterodera* species from soils by centrifugation in high density solutions. *J. Nematol.* 1:7 (abstr.).
- Evans, K., J. Stafford, R. Webster, P. Halford, M. Russell, A. Barker, and S. Griffin. 1998. Mapping potato cyst nematode populations for modulated applications of nematicides. *Aspects Appl. Biol.* 52:1–8.
- Ferris, H., T.A. Mullens, and K.E. Foord. 1990. Stability and characteristics of spatial description parameters for nematode populations. *J. Nematol.* 22:427–439.
- Francl, L.J. 1986a. Spatial analysis of *Heterodera glycines* populations in field plots. *J. Nematol.* 18:183–189.
- Francl, L.J. 1986b. *Heterodera glycines* population dynamics and relation of initial population to soybean yield. *Plant Dis.* 70:791–795.
- Golden Software. 1999. *User's guide*. Golden Software, Golden, CO.
- Goovaerts, P. 1997. *Geostatistics for natural resources evaluation*. Oxford Univ. Press, New York.
- Huck, M.G., C.M. Peterson, G. Hoogenboom, and C.D. Busch. 1986. Distribution of dry matter between shoots and roots of irrigated and nonirrigated determinate soybeans. *Agron. J.* 78:807–813.
- Journel, A.G., and C.H. Huijbregts. 1978. *Mining geostatistics*. Academic Press, New York.
- Koenning, S.R., S.C. Anand, and J.A. Wrather. 1988. Effect of within-field variation in soil texture on *Heterodera glycines* and soybean yield. *J. Nematol.* 20:373–380.
- Koenning, S.R., and K.R. Barker. 1995. Soybean photosynthesis and yield as influenced by *Heterodera glycines*, soil type and irrigation. *J. Nematol.* 27:51–62.
- Lauritis, J.A., R.V. Rebois, and L.S. Graney. 1983. Development of *Heterodera glycines* Ichinohe on soybean, *Glycine max* (L.) Merr., under gnotobiotic conditions. *J. Nematol.* 15:272–280.
- Lehman, P.S. 1994. Dissemination of phytoparasitic nematodes. *Nematol. Circ.* 208. Florida Dep. of Agric. and Consumer Serv., Div. of Plant Industry, Gainesville.
- Matheron, G. 1963. Principles of geostatistics. *Econ. Geol.* 58:1246–1266.
- McSorley, R., and D.W. Dickson. 1991. Determining consistency of spatial dispersion of nematodes in small plots. *J. Nematol.* 23:65–72.
- Melton, T.A., B.J. Jacobsen, and G.R. Noel. 1986. Effects of temperature on development of *Heterodera glycines* on *Glycine max* and *Phaseolus vulgaris*. *J. Nematol.* 18:468–474.

- Pierce, F.J., and P. Nowak. 1999. Aspects of precision agriculture. *Adv. Agron.* 67:1–85.
- Riggs, R.D. 1987. Nonhost root penetration by the soybean cyst nematode. *J. Nematol.* 19:251–254.
- Robertson, G.P., and D.W. Freckman. 1995. The spatial distribution of nematode trophic groups across a cultivated ecosystem. *Ecology* 76:1425–1432.
- Schabenberger, O., and F.J. Pierce. 2002. Contemporary statistical models for the plant and soil sciences. CRC Press, Boca Raton, FL.
- Seinhorst, J.W. 1967. The relationship between population increase and population density in plant parasitic nematodes. *Nematologica* 13:429–442.
- Seinhorst, J.W. 1982. The distribution of cysts of *Globodera rostochiensis* in small plots and the resulting sampling errors. *Nematologia* 28:285–297.
- [USDA-NRCS Soil Survey Division] Soil Survey Division, Natural Resources Conservation Service, U.S. Department of Agriculture. 2001. Official soil series descriptions [Online]. Available at <http://soils.usda.gov/classification/main.htm> (accessed 23 Mar 2001; verified 31 Mar. 2003). USDA-NRCS Soil Survey Division, Washington, DC.
- Taylor, L.R. 1961. Aggregation, variance and the mean. *Nature* 189:732–735.
- Taylor, L.R. 1984. Assessing and interpreting the spatial distribution of insect populations. *Annu. Rev. Entomol.* 29:321–357.
- Threlkeld, G.W., and J.E. Feenstra. 1974. Soil survey of Shiawassee County, Michigan. USDA Soil Conserv. Serv., Washington, DC.
- Todd, T.C., and C.A.S. Pearson. 1988. Establishment of *Heterodera glycines* in three soil types. *Ann. Appl. Nematol.* 2:57–60.
- Wang, J., P.A. Donald, T.L. Niblack, G. Bird, J. Faghihi, J.M. Ferris, C. Grau et al. 2000. Soybean cyst nematode reproduction in the north central United States. *Plant Dis.* 84:77–82.
- Webster, R., and B. Boag. 1992. Geostatistical analysis of cyst nematodes in soil. *J. Soil Sci.* 43:583–595.
- Webster, R., and T.M. Burgess. 1980. Optimal interpolation and isarithmic mapping of soil properties: III. Changing drift and universal kriging. *J. Soil Sci.* 31:505–524.
- Workneh, F., E. Villanueva, and C.M. Rush. 2001. Relative within-field distribution patterns of beet necrotic yellow vein virus and beet soilborne mosaic virus. *Phytopathology* 91:S96 (abstr.).
- Workneh, F., X.B. Yang, and G.L. Tylka. 1999. Soybean brown stem rot, *Phytophthora sojae*, and *Heterodera glycines* affected by soil texture and tillage relations. *Phytopathology* 89:844–850.
- Wrather, J.A., T.R. Anderson, D.M. Arsyad, Y. Tan, L.D. Ploper, A. Porta-Puglia, H.H. Ram, and J.T. Yorinori. 2001a. Soybean disease loss estimates for the top ten soybean-producing countries in 1998. *Can. J. Plant Pathol.* 23:115–121.
- Wrather, J.A., W. Stienstra, and S.R. Koenning. 2001b. Soybean disease loss estimates for the United States from 1996 to 1998. *Can. J. Plant Pathol.* 23:122–131.
- Young, L.D. 1992. Epiphytology and life cycle. p. 27–36. *In* R.D. Riggs and J.A. Wrather (ed.). *Biology and management of the soybean cyst nematode*. The Am. Phytopathol. Soc., St. Paul, MN.
- Young, L.D. 1998. Influence of soybean cropping sequences on seed yield and female index of the soybean cyst nematode. *Plant Dis.* 82:615–619.
- Young, L.D., and E.E. Hartwig. 1992. Cropping sequence effects on soybean and *Heterodera glycines*. *Plant Dis.* 76:78–81.